

# Behavioral Analysis of Turbulent Exhale Flows

Shane Transue<sup>†</sup>, Sayed Mohsin Reza<sup>†</sup>, Ann C. Halbower<sup>‡</sup>, and Min-Hyung Choi<sup>†</sup>

**Abstract**—Dense exhale flow through  $CO_2$  spectral imaging introduces a pivotal trajectory within non-contact respiratory analysis that consolidates several pulmonary evaluations into a single coherent monitoring process. Due to technical limitations and the limited exploration of respiratory analysis through this non-contact technique, this method has not been fully utilized to extract high-level respiratory behaviors through turbulent exhale analysis. In this work, we present a structural foundation for respiratory analysis of turbulent exhale flows through the visualization of dense  $CO_2$  density distributions using precisely refined thermal imaging device to target high-resolution respiratory modeling. We achieve spatial and temporal high-resolution flow reconstructions through the cooperative development of a thermal camera dedicated to respiratory analysis to drastically improve the precision of current exhale imaging methods. We then model turbulent exhale behaviors using a heuristic volumetric flow reconstruction process to generate sparse flow exhale models. Together these contributions allow us to target the acquisition of numerous respiratory behaviors including, breathing rate, exhale strength and capacity, towards insights into lung functionality and tidal volume estimation.

## I. INTRODUCTION

Accurate non-contact respiratory analysis has recently gained popularity within the domains of wireless signal processing [8] and computer vision [12] to automate and significantly broaden the class of quantitative respiratory metrics that non-contact methods can reliably address. Numerous techniques exist for both contact and non-contact respiratory analysis [4], however all of these methods *indirectly* infer breathing behaviors or utilize correlation functions for respiratory analysis. Techniques within computer vision have introduced thermal infrared cameras with spectral filters for  $CO_2$  imaging for respiratory analysis [2], however the applicability of these techniques to comprehensive respiratory analysis is severely underdeveloped and the adoption of these methods has been very limited. This is due to three primary factors shared between most prior vision-based techniques: (1) prior objectives only emphasize simple quantitative measures such as respiratory rate [3] within limited Regions of Interest (RoI) and strength [6], limiting potential high-level behavioral analysis, (2) prior devices lack the sensitivity required to monitor subtle density variances and complex flows behaviors for identifying respiratory conditions, and (3) frame-rate limitations inhibit the ability to accurately capture

<sup>†</sup> This work is partially supported by the DoEd GAANN Fellowship: P200A150283 and NSF Grant: 1602428. S. Transue, S. M. Reza, and M-H. Choi are with the University of Colorado Denver Department of Computer Science and the Comcast Media and Technology Center. Emails: {shane.transue, sayedmohsin.reza, min.choi}@ucdenver.edu

<sup>‡</sup> A. C. Halbower is an MD of Pulmonary Medicine at the University of Colorado School of Medicine and with Children’s Hospital Colorado. Email: ann.halbower@childrenscolorado.org

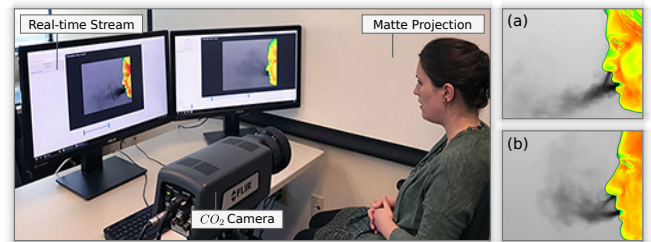


Fig. 1. Dense exhale flow analysis through optimized  $CO_2$  imaging for illustrating unique respiratory behaviors of multiple individuals (a-b).

rapid and turbulent respiratory behaviors. To develop a device for directly analyzing turbulent  $CO_2$  exhale flows [3], we have coordinated the development of a *hyper*-sensitive FLIR thermal camera that contains an embedded spectral filter that directly targets the  $CO_2$  spectral band (3-5[ $\mu m$ ]). From our requirement specification<sup>1</sup>, the device provides raw  $CO_2$  count images that contain the infrared wavelength activation counts within the  $CO_2$  absorption band [10], [11]. Through the development these imaging methods and our *direct* measurements of breathing behavior, we introduce a new vector in vision-based clinical respiratory analysis. This includes direct flow and thermal analysis for subtle alternations in airflow related to asthma, Chronic Obstructive Pulmonary Disease (COPD), developmental conditions related to nose and mouth breathing distributions, cognitive function [13], sleep apnea, and Sudden Infant Death Syndrome (SIDS).

## II. RELATED WORK

The primary evaluation criteria within respiratory analysis revolves around the collection of a limited set of quantitative metrics such as breathing rate, flow analysis, and tidal volume estimates. Extensive research has culminated numerous *contact* [4] and *non-contact* [8], [12] methods that obtain these metrics with promising levels of accuracy. However, based on these existing methods, all current respiratory evaluation is performed using *indirect* methods, that is, they infer measurements through secondary signals such as visible chest movements, vibration, pressure, acceleration, or sound [4]. Prior methods using spectral analysis for  $CO_2$  visualization [3] have introduced a direct means of evaluating respiratory behaviors using *direct* exhale measurements for breathing rate. Similar to this form of direct analysis, we measure and model the exhale flow consisting of the visualized thermal signature of the  $CO_2$  waveform. While prior methods only provide a breathing rate evaluation, this form of visualization is underutilized due to its ability to generate

<sup>1</sup>FLIR A6788sc InSb CCF, 640x512 resolution  $CO_2$  count images @ 30-120[fps] with programmatic camera control and raw data acquisition.

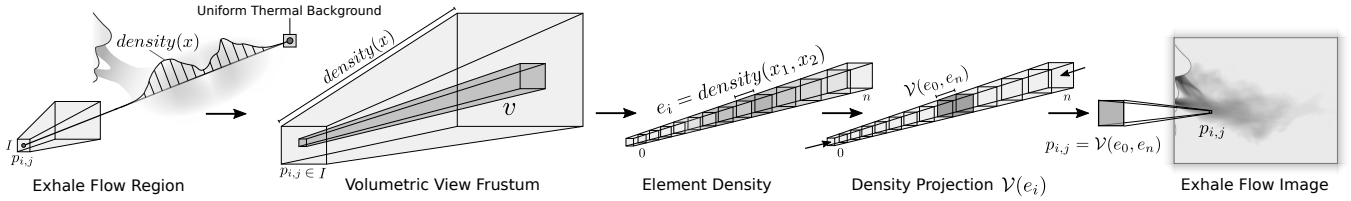


Fig. 2. Volumetric and density modeling of the  $CO_2$  exhale region defined by the view frustum of the imaging device. The exhale flow region contains a non-linear  $CO_2$  concentration distribution function  $density$  over distance  $x$ . Each individual pixel  $p_{i,j}$  represents a continuous volume through which the exhale flows. Based on the density value evaluated at each element  $e_i$ , the final value of pixel  $p_{i,j}$  is the projection of all element densities within  $v$ .

numerous additional metrics such as nose/mouth distribution, velocity, dissipation, behavioral characteristics and even insight into lung efficiency in controlled environments. To enable these metrics, the result of our work significantly diverges from existing  $CO_2$ -based imaging techniques [2], [3] in both the level of analysis and the resolution of our modeling, as shown in Figure 3 (b), as compared with the prior result introduced within [3] shown in Figure 3 (a).

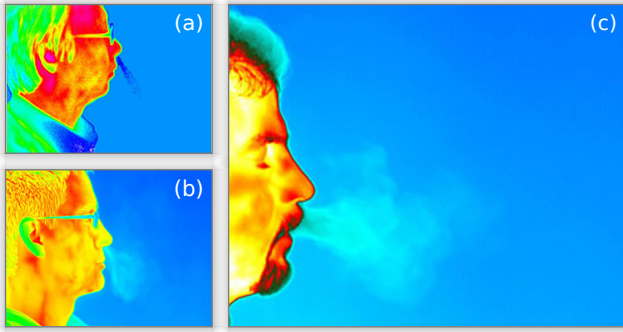


Fig. 3. Thermal respiratory  $CO_2$  imaging: (a) results from [3], compared with our direct reconstruction in of the experimental setup in (b), with a detailed example of our exhale visualization result in (c).

Evaluating objective reconstructions of vortex behaviors within turbulent flows is an open problem within computational fluid dynamics due to reference frame dependent flow behaviors. Recent flow visualization techniques have proposed visualizations of vortex behavior through optimally local reference frame optimization [5] for reconstructing complex vortex flows. Other flow reconstruction techniques attempt to build models of complex gas flows through refraction-based Background-oriented Schlieren methods [9] or through Light-Path approximations captured through multiple imaging devices using visible light wavelength [7]. These techniques represent a divergence from traditional tracer-based method such as Particle Image Velocimetry (PIV) that requires discrete cross-correlation of discrete tracer particles which is impractical for our clinical domain.

Due to the limitations of the clinical domain, these tracer and light-based, fixed environmental constraints are impractical, therefore we introduce a heuristic-based model for analyzing turbulent respiratory exhale flows. Based on this contribution, we build a framework that: (1) provides an accurate turbulent exhale flow analysis, (2) model direct flow behaviors are required for identifying potential respiratory conditions, and (3) introduce a new methodology for identifying condition-trait signatures using clinical non-contact respiratory analysis with an aim of associating exhale flow behaviors with common pulmonary conditions and diseases.

### III. METHOD

Exhale flow behavior modeling provides a basis for evaluating high-level respiratory characteristics based on a set of observable phenomena that is not facilitated by current monitoring techniques. This includes momentary fluctuations within exhale streams that inherently contribute to secondary flow behaviors associated with obstructed breathing, subtle changes between nose-mouth breathing distributions, lung functionality, and the ability to identify abnormal exhale  $CO_2$  signatures. To extend respiratory analysis to include these metrics, we introduce a dense flow reconstruction process including: (1) flow estimation through dense optical flow, (2) heuristic-based flow slice extrapolation, and (3) provide a volumetric sparse scalar field representation of recorded exhale behaviors for extended monitoring periods.

#### A. Dense Exhale Modeling

Carbon dioxide density images obtained through our camera are characterized by the projection of volumetric densities of the observable gas flows with general infrared radiation, filtered to the spectral wavelength interval required for  $CO_2$  imaging. To maximize clarity in this measurement, we improve the sensitivity of our recording model by adding a thin matte surface parallel to the imaging plane that contains a uniform heat distribution. Through the view frustum of the camera shown in Figure 2, we model the continuous volume  $v$  of pixel  $p_{i,j}$  from this surface to the image plane  $I$  as a discrete set of  $n$  elements with an unknown density distribution function  $density$  as a function of distance  $x$ . This per-element density function  $V(e_i)$  is projected to pixel  $p_{i,j}$  resulting in an irreversible loss of this distribution. Our model is based on heuristic approximations of the inverse  $\mathcal{V}^{-1}(e_i)$  of this volumetric projection to determine the per-frame scalar density value  $v_{i,j,k}$  within a sparse voxel grid:

$$v_{i,j,k} = \mathcal{V}^{-1}(p_{i,j}) = \mathcal{V}^{-1} \left[ \sum_{i=1}^n density(e_i) \right] \quad \forall p \in I \quad (1)$$

Since the consolidation of this density volume to an image representation is *unrecoverable* due to the projection of the per-element densities, the reconstruction is inherently limited to an approximation of the original volume but preserves overall flow behavior. Figure 4 illustrates the resulting intensity images of the exhale obtained through this method, demonstrating multiple dense turbulent flows. Due to this result, we do not limit our analysis to a sub-image RoI, rather we consider the entire exhale region to model both behavioral characteristics and diffusion properties of exhale sequences to build a per-patient respiratory profile.



Fig. 4. Recorded turbulent exhale flow from the mouth (left), nose (center), and both nose and mouth simultaneously (right). Through our imaging process, we obtain an accurate illustration of the  $CO_2$  density distribution and flow behavior with minimal background interference.

### B. Dense Flow Reconstruction

Dense flow reconstruction from two-dimensional imaging is inherently ambiguous and cannot be directly recovered. To approximate a resulting distribution of the flow within a reconstruction we employ a four step process for estimating exhale density flow behaviors based on consecutive  $CO_2$  image pairs over time and space, outlined in Figure 5.

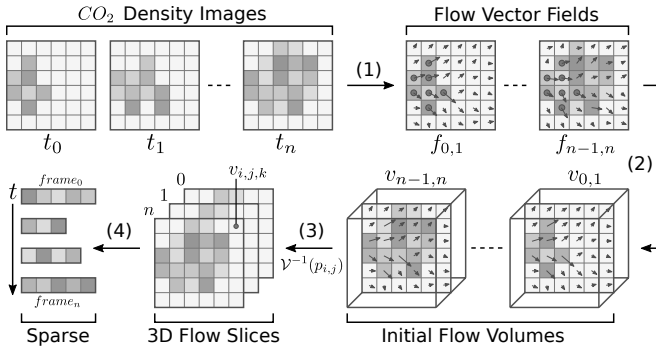


Fig. 5. Exhale flow reconstruction process. We approximate the reconstruction of the projected density volume by estimating the function  $density(x)$  using heuristic approximations.

In this process we collect the set of  $n$  density images over time  $t$ , (1) compute the apparent flow through dense optical flow [1], (2) emplace these flow frames into a volumetric voxel grid as a seed slice in the middle of this volume, (3) extrapolate slice flow estimates, and (4) convert these scalar fields into sparse representations for each frame. The sparse representation is due to the dense resolution of the volumetric grid, which encodes the density value, and flow vector of each cell. We evaluate each frame independently within this single compute volume. This results in an  $n$  frame recording, each composed of a sparse 3D scalar field that approximates disjoint flow behaviors recorded in each frame.

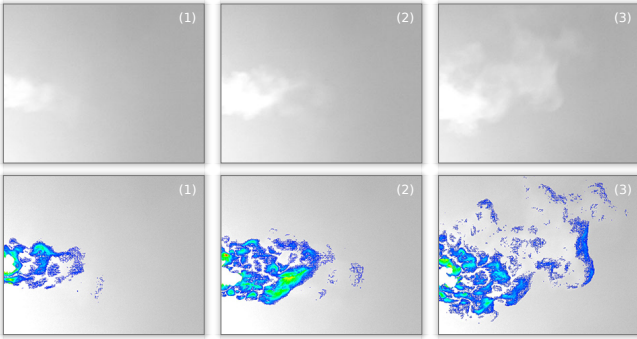


Fig. 6. Turbulent exhale optical flow vectors. The generated vector field illustrates the *apparent* flow computed through a standard dense optical flow algorithm. The (top) row illustrates the original  $CO_2$  density images, and the (bottom) row illustrates the resulting vector norm-color-mapped flow.

## IV. EXPERIMENTAL RESULTS

The primary objective of flow-based respiratory analysis is to detect abnormalities within normal breathing based on the cross-sectional view of the exhale without the interference of background sources of infrared radiation. Since the objective of our reconstruction is to identify minute changes in the turbulent flow of an individual's exhale, we assume ideal posture and exhale region with a projection screen matte background. To focus the region to the exhale volume, we refine our region of interest to exclude the face, but do not limit our analysis to a region of interest. In Figure 9 we present two six-frame segmented exhale flow sequences.

### A. Behavioral Analysis of Exhale Traits

The results of the proposed method present both flow visualization and approximated volumetric flow reconstruction to evaluate exhale strength and velocity shown in Figure 7, nose-mouth distribution, strength, and minute flow variances that can be associated with abnormal breathing. These contributions will greatly broaden the horizon of exhale analysis over existing frequency-based methods that utilize Fourier transforms to directly compute breathing rate.

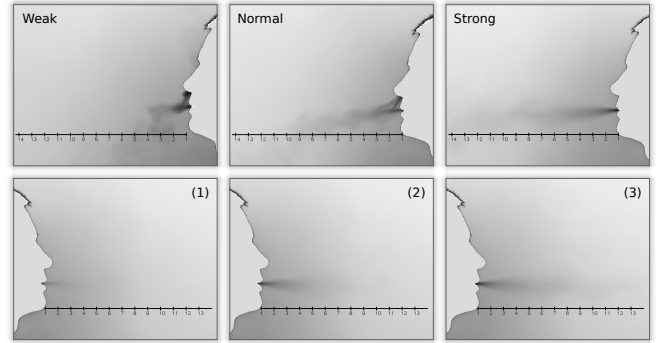


Fig. 7. Resulting videos for weak, normal, and strong exhale strengths (top row). In exhale velocity, we differentiate per frame for slow, normal, and fast velocities (bottom row), as a function of the exhale speed,  $CO_2$  concentration, and the environmental thermal dissipation rate.

Quantitatively, we express the relative nose-mouth distribution as an estimated contribution to the exhale. For the velocity component, we express the change in exhale length over time as a result of exhaled  $CO_2$  concentration.

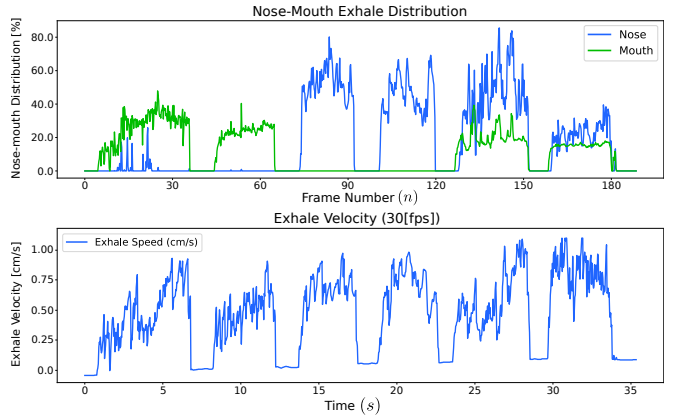


Fig. 8. Exhale nose-mouth distribution (top) for two exhales in each configuration: mouth, nose, and simultaneous oral-nasal breathing. The exhale velocity plot (bottom) demonstrates exhale characteristics for distance, strength, and the dissipation factor linked to  $CO_2$  concentration.

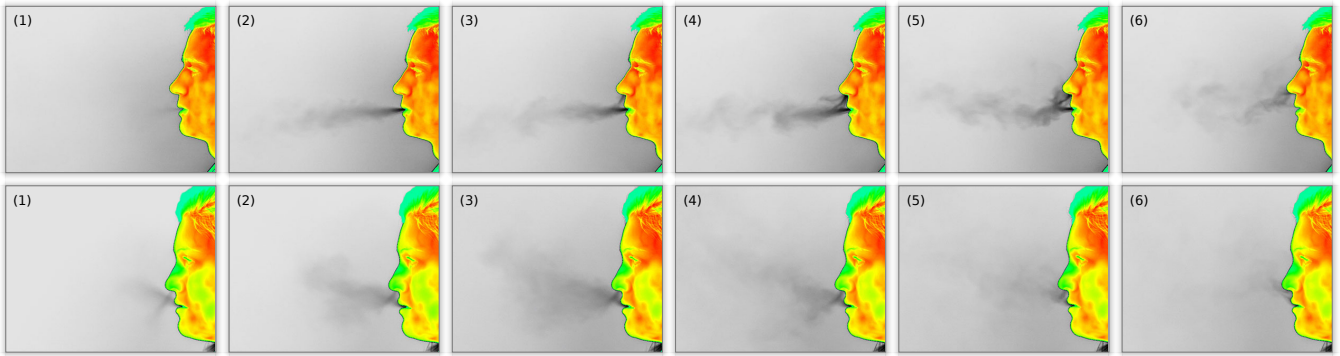


Fig. 9. Resulting  $CO_2$  density distribution images illustrating unique respiratory patterns between individuals (top vs bottom rows). For each image sequence, one exhale period has been recorded and visualized, showing the clear separation between the nose-mouth distribution and density flow behaviors. These flow behaviors unique to each individual are subject to their own physiology and can be evaluated to identify per-individual exhale traits.

### B. Flow Reconstruction

The extrapolation of our flow analysis into our 3D sparse scalar field is segmented by the optical flow vector norms. This cleanly separates the exhale densities from the residual general interference from background sources and natural environmental airflow. Using this technique, we can completely reconstruct segmented exhale behaviors. The resulting reconstruction is rendered as volumetric clouds within Figure 10.

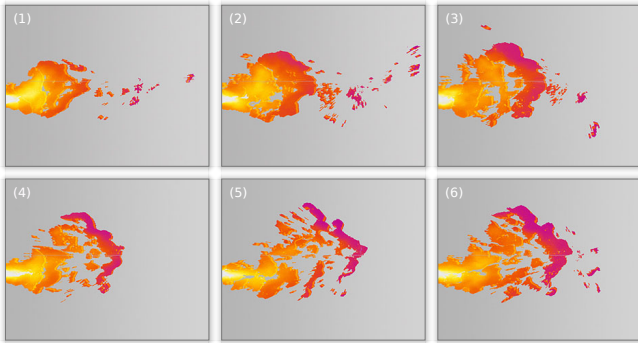


Fig. 10. Reconstructed 3D sparse exhale flow sequence rendered as a color-mapped sparse cloud (from top-left to bottom-right). Our framework incorporates interchangeable heuristics for extrapolating 3D flow fields.

## V. EVALUATION AND DISCUSSION

Turbulent flow analysis is inherently complex. Differentiating intersecting flows further complicates this analysis for nose/mouth separation. Accurate 3D reconstruction of volumetric flows without depth measurements or advection is also intangible. To preserve validity of our model, we focus on maintaining flow behavior characteristics, but do not formulate an exact volumetric exhale reconstruction. Rather, this form of  $CO_2$  exhale imaging opens up a new medical significance in the monitoring of normal versus pathological airflow from the lower and upper airways. Volume measurements quantify lung capacity or effect of therapy in pulmonary patients with common medical problems such as asthma and chronic obstructive pulmonary disease without the need to utilize bulky pulmonary function machines with the required patient cooperation. Subtle alterations of airflow velocity and nose-mouth distribution can determine upper airway obstruction or those at risk for sleep apnea or sudden infant death. With the ability to monitor subtle changes in

airflow in infants sleeping prone versus supine or in car seats or soft bedding, the advancement of research into the cause and prevention of SIDS cases achieves a new trajectory in high-resolution  $CO_2$  respiratory behavioral analysis.

## VI. CONCLUSION

In this work we have coordinated the development of a  $CO_2$  imaging and respiratory monitoring framework that facilitates the recording and modeling of dense exhale flow behaviors. This non-contact, direct method establishes the foundation for a respiratory monitoring solution that includes new metrics for: rate, strength, nose/mouth distribution, condition trait identification, and volumetric modeling. This framework will be used to establish extensive patient studies utilizing diverse exhale quantitative metrics as future work.

## REFERENCES

- [1] J. L. Barron, D. J. Fleet, and S. S. Beauchemin. Performance of optical flow techniques. *Intl. Journal on Comp. Vision*, 12(1):43–77, 1994.
- [2] J. Fei and I. Pavlidis. Analysis of breathing air flow patterns in thermal imaging. In *Engineering in Medicine and Biology Society, 2006. EMBS'06*, pages 946–952. IEEE, 2006.
- [3] J. Fei, Z. Zhu, and I. Pavlidis. Imaging breathing rate in the  $CO_2$  absorption band. In *Engineering in Medicine and Biology*, 2005.
- [4] A. R. Fekr et al. Design and evaluation of an intelligent remote tidal volume variability monitoring system in e-health applications. In *IEEE J. of Biomedical and Health Informatics*, 2015.
- [5] T. Günther, M. Gross, and H. Theisel. Generic objective vortices for flow visualization. *ACM Transactions on Graphics (Proc. SIG-GRAPH)*, 36(4):141:1–141:11, 2017.
- [6] D. Hanawa, T. Ohguchi, and K. Oguchi. Basic study on non-contact measurement of human oral breathing by using far infra-red imaging. In *Telecommunications and Signal Processing (TSP), 2016 39th International Conference on*, pages 681–684. IEEE, 2016.
- [7] Y. Ji, J. Ye, and J. Yu. Reconstructing gas flows using light-path approximation. In *Computer Vision and Pattern Recognition*, 2013.
- [8] P. Nguyen, S. Transue, M.-H. Choi, A. C. Halbower, and T. Vu. Wikispiro: Non-contact respiration volume monitoring during sleep. In *Proceedings of the Eighth Wireless of the Students, by the Students, and for the Students Workshop*, S3, pages 27–29, 2016.
- [9] M. Raffel. Background-oriented schlieren (bos) techniques. *Experiments in Fluids*, 56(3), Mar 2015.
- [10] R. Rehm et al. Dual-colour thermal imaging with inas/gasb superlattices in mid-wavelength infrared spectral range. *Electronics Letters*, 42(10):577–578, 2006.
- [11] F. Rutz et al. Imaging detection of  $CO_2$  using a bispectral type-ii superlattice infrared camera. In *Quant. InfraRed Thermo.*, 06 2012.
- [12] S. Transue et al. Real-time tidal volume estimation using iso-surface reconstruction. In *IEEE CHASE'16*, pages 209–218, 2016.
- [13] C. Zelano et al. Nasal respiration entrains human limbic oscillations and modulates cognitive function. *Neurosci*, 7(49), 2016.